ANL-HEP-TR-96-71
91135

ASYMMETRIES IN INCLUSIVE PION PRODUCTION AT LARGE x_F = (0.5 TO 0.8) AND $p_T \geq 0.8$ GeV/c WITH A POLARIZED BEAM FOR A RHIC POLARIMETER♦

by

K. Krueger, T. LeCompte, H. Spinka, D. Underwood, and A. Yokosawa

High Energy Physics Division
Argonne National Laboratory, Argonne, Illinois 60439 USA

G. Bunce, H. Huang, Y. Makdisi, F. Mariam, T. Roser, M. Syphers

Brookhaven National Laboratory
Upton, New York 11973 USA

N. I. Belikov, A. M. Davidenko, A. A. Derevschikov, S. V. Erin, S. B. Nurushev, Yu. A. Matulenko, A. I. Pavlinov, A. N. Vasiliev

IHEP, Institute for High Energy Physics
Protvino, Russia

I. G. Alekseev, V. P. Kanavets, D. N. Svirida

Institute for Theoretical and Experimental Physics (ITEP)
Cheremushkinskaya 25, 117259 Moscow, Russia

M. Bai*, S. Y. Lee

Indiana University
Bloomington, Indiana 47405

26 August 1996

Spokespersons: Y. Makdisi, A. Yokosawa

♦ Work supported in part by the U.S. Department of Energy, Division of High Energy Physics, Contract W-31-109-ENG-38.

* Also Argonne National Laboratory

ABSTRACT

We propose to measure asymmetries in the inclusive reactions,

$$p^{\uparrow}p \rightarrow \pi^{+} \text{ anything}, \; p^{\uparrow}C \rightarrow \pi^{+} \text{ anything},$$

$$p^{\uparrow}p \rightarrow \pi^{-} \text{ anything}, \; p^{\uparrow}C \rightarrow \pi^{-} \text{ anything}$$

using a transversely polarized beam, a liquid hydrogen target, and a carbon target. The measurements would be made using the 23-GeV/c proton beam in an extracted beam line from the AGS, a spectrometer consisting of an analyzing magnet, scintillation hodoscopes, scintillation trigger counters, and a gas threshold Cerenkov counter. The kinematic range covered by the experiments would be p_T up to 1.0 GeV/c and $x_F = p_L^* / p_{max}^* \approx 0.5$ to 0.8.

The purpose of this proposal is to obtain basic information in order to design a polarimeter for the RHIC polarized beams. The RHIC polarimeter is a crucial item for the success of the RHIC spin program.

Introduction

At RHIC we plan to collide polarized protons with beam energies ranging from 23 GeV (at injection) to 250 GeV. Polarimeters which have been used at lower energies, such as the AGS internal polarimeter, use proton-proton elastic scattering to analyze the beam polarization. The analyzing power for this reaction (usually at fixed transverse momentum, or -t = .15 to . 3 $(\text{GeV/c})^2$) decreases inversely with the beam momentum, becoming too small to be useful much above 23 GeV/c. We plan, instead of p-p elastic scattering, to use inclusive pion production to analyze the polarization of the RHIC beams.

Fermilab E-704 used a proton beam with known polarization derived from lambda hyperon decay to measure the analyzing power for charged pion production, for 200-GeV/c incident protons.[1] The analyzing power is large for large p_T (Fig. 1 has p_T between .7 and 2.0 GeV/c), as is the production cross section, offering an ideal reaction for RHIC polarimetry. The analyzing power for this reaction is absolutely calibrated, via the well-known lambda-decay asymmetry parameter alpha, to 6% of itself at 200 GeV/c.[1]

We expect that the analyzing power for pion production is largely energy independent over the RHIC energy range, with significant analyzing power also at injection energy, or 23-GeV/c momentum. We observe that i) the analyzing power for π^+ production[2] at the ZGS (12 GeV/c) had the same magnitude at large x_F and a similar kinematic dependence (see Fig. 2) as at 200 GeV/c and ii) there are phenomenological models which connect pion asymmetry and hyperon polarization in production, and existing hyperon polarization data are essentially independent of energy. However, the π^- data[2] at 12 GeV/c do not exhibit the same behavior (see Fig. 2) as at 200 GeV/c. We would particularly like to know how the π^- data at 23 GeV/c behave. We would prefer that the RHIC polarimeter use π^- asymmetry to avoid having to do particle identification.

We propose to measure both π^+ and π^- asymmetry, produced by the polarized AGS beam at 23 GeV, the injection energy for RHIC. (This injection energy avoids a large spin resonance at the AGS, and is above the RHIC transition energy.) The most important issue to resolve is whether there is significant analyzing power for π^+ and/or π^- production at 23 GeV/c. We will calibrate the beam polarization using proton-proton elastic scattering from the AGS internal polarimeter, which uses a hydrocarbon target, and also with the extracted beam using a liquid hydrogen target. This will give an absolute calibration of the proton polarization to 11% of itself. (This calibration is based on experiments with polarized targets where the target polarization is well-measured.)

This measurement at the AGS, along with the 200-GeV/c measurement from Fermilab (E-704), will give us two calibrated energies for the RHIC polarimeter. We plan to connect asymmetries measured at other energies by accelerating (or decelerating) to 200 GeV/c to absolutely determine the RHIC beam polarization. One can also do this for the 23-GeV/c analyzing power, but we feel it is crucial to start the process of commissioning the polarized beam at RHIC with a known (and significant) analyzing power at the injection energy. In addition, if the analyzing power at 23 GeV/c is similar to 200 GeV/c, we will initially interpolate to obtain the analyzing power at intermediate energy, for commissioning purposes.

The E-704 asymmetry measurements used a hydrogen target. The ZGS data shows no difference in the analyzing power for pions produced from hydrogen and deuterium targets. For the RHIC polarimeter, we will probably use carbon and hydrogen targets at different times, but we start with a carbon target for simplicity. We need to check any difference in analyzing power between hydrogen and carbon targets.

We propose to measure asymmetries from $x_F = 0.5$ to 0.8 and $p_T = 0.8.$ to 1.0 GeV/c in the processes:

$$p^{\uparrow}p \rightarrow \pi^{+} \text{ anything}, \; p^{\uparrow}C \rightarrow \pi^{+} \text{ anything},$$

$$p^{\uparrow}p \rightarrow \pi^{-} \text{ anything}, \; p^{\uparrow}C \rightarrow \pi^{-} \text{ anything}$$

at 23 GeV/c with special emphasis on the high-x_F region, where appreciable asymmetries were observed at 200 GeV/c.[1] The experiment will utilize a transversely polarized beam, and thus we will measure the asymmetry

$$A_n(x_F, p_T) = \frac{E\, d^3\sigma_{\uparrow} / dp^3 - E\, d^3\sigma_{\downarrow} / dp^3}{E\, d^3\sigma_{\uparrow} / dp^3 + E\, d^3\sigma_{\downarrow} / dp^3},$$

where $E\, d^3\sigma/dp^3$ is the invariant cross-section for particle production and $\uparrow$, $\downarrow$ refer to the polarization direction of the incoming proton.

Experimental Technique

The proposed layout of the experimental apparatus is shown in Fig. 3.

The transversely polarized proton beam is incident upon a 25-cm long liquid hydrogen target. The production angles of charged particles emerging from the target are measured in the scintillation hodoscopes, H_1 (16 ctrs., 31 segments (segment = 2 mm)) and H_2 (16 × 16 ctrs, 31 × 31 segments). Their angles, after magnetic analysis, are again measured in the hodoscopes, H_3 (24 × 24 ctrs., 47 × 47 segments) and H_4 (28 × 28 ctrs., 55 × 55 segments). We will need an H magnet with a 30 inch width, 6 inch height and p_T kick of 1.0 GeV/c.

For π^- production, particle identification is simple due to the opposite curvature of pions and protons in the field of the bending magnet.

For π^+ production, particle identification is more difficult. Scattered protons are expected to be more numerous than π^+. The π^+ trigger will be tightened by requiring the threshold Cerenkov counter with eight-inch diameter aperture in coincidence. A coincidence between counters S1, S2, and S3 forms the most basic element of our trigger. There is a hole counter marked HV in Fig. 3 to limit the beam size. It has four segments, VUL, VUR, VDL, and VDR. A trigger logic diagram is shown in Fig. 4. The coincidence will use 10 nsec overlap, and the accidental rate will be small.

Monte Carlo studies show that we can veto approximately half of the low p_T events that lie within our acceptance. Figure 6 is a correlation plot between X positions in hodoscopes two and four. On the left of the figure we have a low p_T cut, and on the right a high p_T cut. We will veto events in the upper left corner, which is almost entirely free of high p_T events and populated by low p_T events.

The hodoscopes will be latched and read out by a PC with an expected 5 msec dead time. A data acquisition block diagram is shown in Fig. 5.

Rates, Resolution, and Run Plan

Invariant cross-sections are given by:

$$E\frac{d^3\sigma}{dp^3} = E\frac{d^3\sigma}{d\phi\, dp_z\, p_T\, dp_T} \quad .$$

$$I_{protons} = \frac{\#\text{ of events} \bullet x_F}{\left(E\frac{d^3\sigma}{dp^3}\right)\left(\frac{\text{protons}}{\text{cm}^2}\right) p_T \bullet \Delta p_T \bullet \Delta x_F \bullet \Delta\phi}$$

where $I_{protons}$ is the total number of protons on target to obtain the desired number of events. p_T and x_F are for the produced pion. $\Delta\phi$ was calculated by a simulation to be 0.19.

The error in the asymmetry is given by $\Delta A_N = \frac{1}{P\sqrt{N}}$, where P is the beam polarization and N is the number of events. Based on Figs. 1 and 2, we expect $A_N = 0.15$. To obtain an error in the asymmetry of $\pm$ 0.006, assuming $P_{beam} = 0.5$ for this run (E-880 intends to achieve 0.7 for injection into RHIC), 10^5 events in a bin are required. We use bin sizes of $\Delta x_F = 0.1$ and Δp_T =.1 GeV/c, and plan four running conditions; π^+, π^-, and two different magnetic fields to cover

$x_F = 0.5$ to 0.8 and $p_T \geq .8$ GeV/c. We will use a beam of 2×10^7 polarized protons per pulse and 1,000 pulses per hour. The cross sections and required hours are given in the following table.

Table 1

$$E\frac{d^3\sigma}{dp^3}\ \left(\text{mb} / \text{GeV}^2\right)$$

X_F	.5	.6	.7	.8	**Running Time H**	**Running Time C**
π^+	.4	.2	.08	.01	10 hours	10 hours
π^-	.2	.07	.03	.006	30 hours	30 hours

The cross sections in the table above are estimated from graphs in Reference 7. They use X_R and

$$X_R = \frac{E^*}{E_{max}{}^*} \approx \frac{P^*}{P_{max}{}^*} = x_F$$

The required running time is about forty hours for each target. The rate in the $x_F = .6$ to .7, $p_T = .8$ to .9 GeV/c, bin is estimated to be 5 to 15 events/spill. The total number of triggers per spill will be 50 to 150. The carbon target will be 1.5 cm in length. The experiment is limited by computer dead time which is 31% at 100 events/spill.

The x_F and p_T resolutions are given in Table 2 below.

Table 2

	$p_T = .8$ GeV, $x_F = .6$		$p_T = 1.0$ GeV, $x_F = .7$	
	No Beam Div.	With Beam Div. $\Delta\theta = 1.5$ mrad	No Beam Div.	With Beam Div. $\Delta\theta = 1.5$ mrad
Δx_F (FWHM)	~ 0.015	~ 0.015	~ .02	~ .02
Δp_T (FWHM) in GeV/c	~ 0.03	~ 0.04	~ .04	~ .05

Plots of the resolution for several variables are given in Figs. 7-10. The acceptance for two different magnet settings is shown in Figs. 11-12.

The cross-section for low p_T events is much greater than for high p_T. We need a magnet that has a p_T kick of at least 1 GeV/c to minimize the number of low p_T triggers. The importance of a large p_T kick is shown in Figs. 11 and 12. These are plots of acceptance, weighted by an experimentally determined differential cross-section for a low p_T kick (Fig. 11), and a large p_T kick (Fig. 12). Acceptance is increased at high x_F and high p_T for a large p_T kick and acceptance is decreased at low x_F and p_T.

Systematic errors could come from a misalignment of the actual beam with the survey line or from a large beam divergence. Both of these conditions could lead to errors in the measurement of p_T. We will minimize the misalignment of the actual beam, and the beam line, by the use of SWIC1 and SWIC2 shown in Fig. 3. Beam divergence will be kept below 1.5 mrad (FWHM) to minimize resolution errors from this source by careful beam transport from the AGS to the beam line.

Background

For π^+ there will be five times as many protons within our acceptance. If 1% of protons are misidentified as pions, protons will make a background trigger rate 5% of the pion trigger rate. Protons will therefore cause no more than a 5% contamination of the pion signal.

The ratio of $\overline{p}$ to π^- is estimated at .03 ± .01. Even without Cerenkov identification the pion signal will have less than 6% contamination from this source. The ratio of K^- and π^- is estimated at .015 ± .015. Again, even without Cerenkov separation of pions and kaons, the pion signal will be contaminated by less than 6% kaons.

Beam Polarization Measurement - pp Elastic Scattering

We will also measure pp elastic scattering around $t = -.15\ (GeV/c)^2$. There are two reasons for doing this. One is to provide an accurate measure of the beam polarization for the inclusive pion experiment. The second reason is to provide a cross-check of the internal AGS polarimeter, which measures the left-right asymmetry of pp elastic scattering between the proton beam and hydrogen in a nylon fishline target.[5] The analyzing power for pp elastic scattering (A_N (pp)) is proportional to $1/p_{lab}$ for fixed momentum transfer, t. A_N (pp) has a broad maximum around $-t = .15\ (GeV/c)^2$ and A_N (pp) = 0.032 ± 0.003 at 24 GeV/c (see Fig. 13). This was measured using a polarized target with known polarization. The combined statistical and systematic error is $\Delta A_N (pp)/A_N (pp) = \pm 11\%$, which will then be the systematic error limit for our pion measurement at 23 GeV/c.

As shown in Fig. 3, recoil-arm detectors and forward counters will be provided for pp elastic scattering. Each recoil arm consists of scintillation counters (SL1, SL2, SR1, SR2) with four phototubes, (ADC's and TDC's are providing pulse heights and time differences to locate a track point in a scintillator), an aluminum absorber wedge (A in Fig. 3), a thick scintillation counter to measure stopped protons (SL3 and SR3 which have dimensions of 5 cm by 8 cm and are 1 m from the beam line), and a veto counter to suppress pions (RV and LV). A similar technique is used for the present internal polarimeter. Additionally, we will measure the momentum of the forward protons with the same magnet used for the pions and detect the forward protons with scintillators F1 and F2 (these have dimensions of 7 cm by 3 cm and are 11 m from the target). F1 and F2 will need to be on a moveable platform centered 35 cm apart about the deflected beam. They will have four different positions during the experiment, one for each of two different field strengths and two field directions. Trigger logic is shown in Fig. 14.

The differential cross section is related to the number of events by this relation

$$\text{\# of events} = \frac{d\sigma}{dt} \times (\text{acceptance}) \times (\text{\# of protons/cm}^2) \times \text{beam} \times \Delta t.$$

The rates are estimated by taking $d\sigma/dt = 5 \times 10^{-26}\ \text{cm}^2/(\text{GeV/c})^2$, acceptance = .013, beam = $2 \bullet 10^7$/spill, $\Delta t = .05\ (\text{GeV/c})^2$ and we will use scintillators to look at the middle 2 cm length of the target to give 8×10^{22} protons/cm^2. This gives an event rate of 50 per spill in each arm. The dead time would be 31% (5 msec × 100/1.6s). We will restrict the distance in the target in the beam direction to 1 or 2 cm by means of trigger or veto scintillators in order to adequately define the recoil angle.

The beam polarization is given by the formula

$$\langle P_{beam} \rangle = \frac{\varepsilon}{A_N}$$

where

$$\varepsilon = \frac{N^+ - N^-}{N^+ + N^-}$$

N^+ and N^- are the normalized number of elastic scatters with spin up and spin down, respectively. The error in the polarization measurement is

$$\left(\frac{\Delta P_{beam}}{P_{beam}}\right)^2 = \left(\frac{\Delta A_N(pp)}{A_N(pp)}\right)^2 + \frac{1}{N}\,\frac{1-(A_N(pp)\,P_B)^2}{(A_N(pp)\,P_B)^2}$$

where the two terms on the right hand side of the equation are the systematic and statistical errors respectively, and N is the total number of events. For 2500 spills (2.5 hours), the relative statistical error would be 12% for a beam polarization of 50% ($\Delta P_{beam}/P_{beam} = 0.12$).

Elastic scatters can be identified by standard kinematics such as outlined in Ref. 6.

Normalization

There will be two luminosity telescopes (not shown in Fig. 3) to monitor beam intensity. They will be placed downstream of the target with one up out of the plane of Fig. 3 and one down below the plane. We will also use an ion chamber in the beam as a cross check of the intensity.

Data Acquisition

In order to minimize development time, we will utilize Pentium PC's and single crate dedicated Camac Crate controllers, basically copying the E-880 internal polarimeter setup. The dead time is approximately 5 msec per event.

Data can be backed up to disks on UNIX machines at Brookhaven at the end of each run.

A single Camac Crate will handle the scalers and registers for the pion experiment and the HV controls. The discriminators with ECL output can be in a stand-alone crate where they can be set by hand or with a controller at the beginning of the experiment.

A separate dedicated PC-Camac system will be used for the elastic scattering measurement. Offline software will be developed by the IHEP group.

Summary

These measurements are needed for the development of RHIC polarimetry. Both carbon and hydrogen targets are needed for the pion inclusive results in order to measure the analyzing power of the targets we expect to use in RHIC. This experiment will help us decide whether to build a π^+ or π^- polarimeter, and how to utilize it.

Running Time Requests

We need to split the running time into runs with two magnet polarities in order to do π^+ and π^-. We further need to split the time with two magnet currents at each polarity to cover the kinematic region of interest. The experiment could in principle be done in eight days in one running period if the beam polarization is high and all goes well. We are asking for an additional later, eight day period, to cover possible problems in either aspect. We also need parasitic beam time to get all the system working.

We assume that we can do the elastic scattering beam polarization measurement concurrently with the pion production off hydrogen. This requires a wide aperture spectrometer magnet. The carbon running requires removal of the hydrogen target. We would like to remove it vertically, in order not to interfere with the recoil arm setup.

In order to utilize the elastic measurement of the beam polarization effectively for the carbon target runs, we will alternate carbon and hydrogen running, so that elastic runs are close in time to the carbon runs. This assumes rapid removal and insertion of the hydrogen target.

We would also like to cross-calibrate the internal AGS polarimeter with the elastic measurement either by running the internal polarimeter for the last 100 ms of each spill, or by using a percentage of the machine cycles for the internal measurement. This would not be done for all the running time.

Location:	External beam line B1
When:	At the end of full-energy polarized beam test (likely in July, 1997)
Tune Up:	Mostly parasitic - 2 weeks before the polarized run

Inclusive $\pi^{\pm}$ production and pp elastic scattering at 23 GeV/c (assuming 50% running efficiency):

i)	Liquid hydrogen	3.5 days	(π^+, π^-, and elastic)
ii)	Carbon	3.5 days	(π^+ and π^-)
iii)	Empty target test	1 day	(π^+, π^-, and elastic)

REFERENCES

1. D. L. Adams et al., Phys. Lett. B264, 462 (1991);
   D. Grosnick et al., to appear in Phys. Rev. D.

2. W. H. Dragoset et al., Phys. Rev. D18, 3939 (1978);
   R. D. Klem et al., Phys. Rev. Lett. 36, 929 (1976).

3. Approved proposal on spin physics using the RHIC polarized collider, Experiment R5.

4. D. G. Crabb et al., Nucl. Phys. B121, 231 (1977).

5. H. Huang et al., Phys. Rev. Lett., 73, 2982 (1994).

6. R. M. Edelstein, Phys. Rev. D5, 1073 (1972).

7. J. R. Johnson et al., Phys. Rev. D17, 1292 (1977).

FIGURE CAPTIONS

Figure 1 Plot of analyzing power at 200 GeV for inclusive pion production from Ref. 1. p_T between .7 GeV/c and 2.0 GeV/c.

Figure 2 Plot of analyzing power at 11.75 GeV for inclusive pion production taken from the data published in Ref. 2. We chose from their tables data for A_N and x_F with p_T between .7 GeV/c and 1.1 GeV/c.

Figure 3 Sketch of the experimental setup for the proposed inclusive pion experiment.

Figure 4 Trigger logic for the pion inclusive experiment.

Figure 5 Data acquisition system.

Figure 6 This is a correlation plot between the x positions in H2 and H4. On the left is a plot of low p_T events and on the right high p_T events. The rectangle in the upper left corner of each plot is marked off to indicate the events we plan to veto. Very few high p_T events are lost, but close to half of the low p_T events are eliminated.

Figure 7 p_T resolution from a Monte Carlo simulation showing the spread of the measured p_T due to the spatial resolution of the hodoscopes.

Figure 8 x_F resolution from a Monte Carlo simulation showing the spread of the measured x_F due to the spatial resolution of the hodoscopes.

Figure 9 From Monte Carlo simulations a track is projected back to z = 0 and the distance from the z-axis is computed. This crudely identifies the track as coming from the target.

Figure 10 This shows where events come from in the target for the kinematic region of interest.

Figure 11 A plot of x_F versus p_T accepted by the apparatus for a wide kinematic range. This has been weighted by an experimentally determined p_T and x_F distribution. This was for a p_T kick of the analysis magnet of .76 GeV/c.

Figure 12 Same as Fig. 10 except the p_T kick is 1 GeV/c. The higher field increases acceptance at higher p_T and x_F.

Figure 13 Plot of analyzing power versus t from Ref. 4.

Figure 14 Trigger logic for the elastic scattering experiment.

APPENDIX A

Equipment Requirements

1. Use of the polarized beam operated in the vertically polarized mode. (BNL)

2. H magnet, 30-inch width, 6-inch gap and hall probe. (BNL)

3. A 25-cm long liquid hydrogen target plus operators on shift. (BNL)

4. A 1.5-cm long carbon target. (BNL)

5. Threshold Cerenkov counter - 8-inch diameter, 2-m long, operated with several atmospheres of freon. (BNL)

6. With the four hodoscopes, beam definition, and luminosity telescopes there are about 200 scintillators. (ANL and IHEP)

7. 15 amplifiers LRS 612A. (ANL and HEEP)

8. 13 discriminators LeCroy 4413. (PREP or HEEP)

9. 5 latches 4448. (ANL, PREP, or HEEP)

10. 7 scalers 4434. (PREP or HEEP)

11. 5 scalers 2551. (ANL and HEEP)

12. 6 channels, visual scalers. (HEEP or PREP)

13. 4 TDC's LRS 2228. (ANL)

14. 4 ADC's 2249. (ANL and HEEP)

15. 5 logic fan/in fan/out 429. (ANL)

16. 10 octal Nim disc 621, 620, etc. (ANL and HEEP)

17. 4 Camac crates. (ANL and HEEP)

18. 6 Nim bins. (ANL and HEEP)

19. 2 Camac interfaces to PC. (ANL)

20. 2 PC's and backup PC. (ANL and HEEP)

21. 2 Printers. (ANL)

22. Ethernet to back up PC disk to UNIX disk (once per run), and also for a local terminal for analysis. (BNL)

23. BNL pre-det module. (BNL)

24. 2 LeCroy 222 or programmable gate modules. (BNL)

25. 8 coincidence modules LRS 365. (ANL and HEEP)

26. Ion chamber in beam for crude beam normalization plus current integrator. (BNL)

27. 2 SWIC's for monitoring beam position. (BNL)

28. 220 channels, HV power supplies, LeCroy 1440 system. (PREP or HEEP)

29. 220 signal cables. (ANL and BNL)

30. 220 high voltage cables. (ANL and BNL)

31. Flat cables. (ANL)

32. 24 phototubes and bases (for elastics). (ANL)

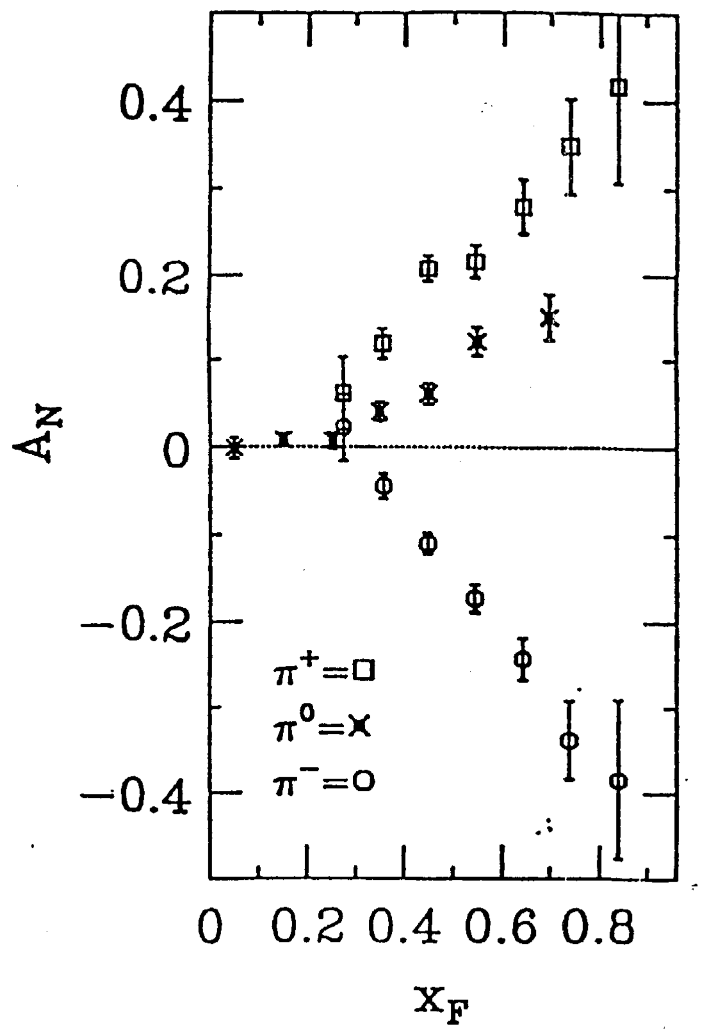

Figure 1

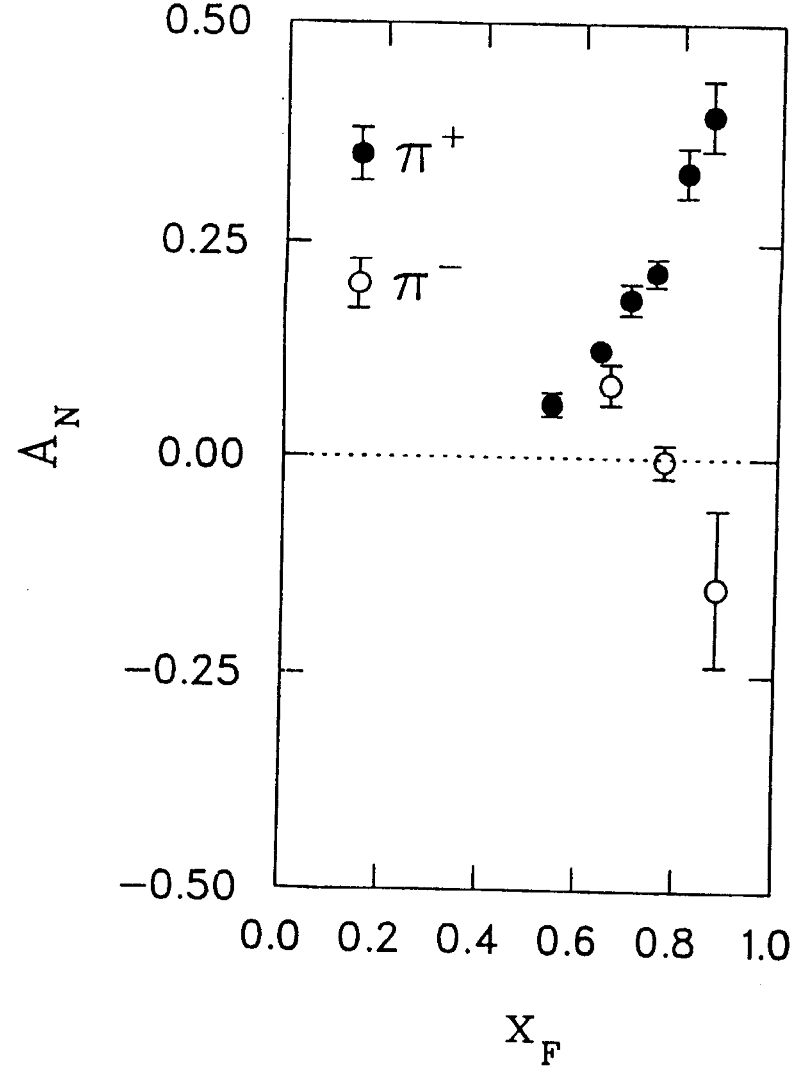

Figure 2

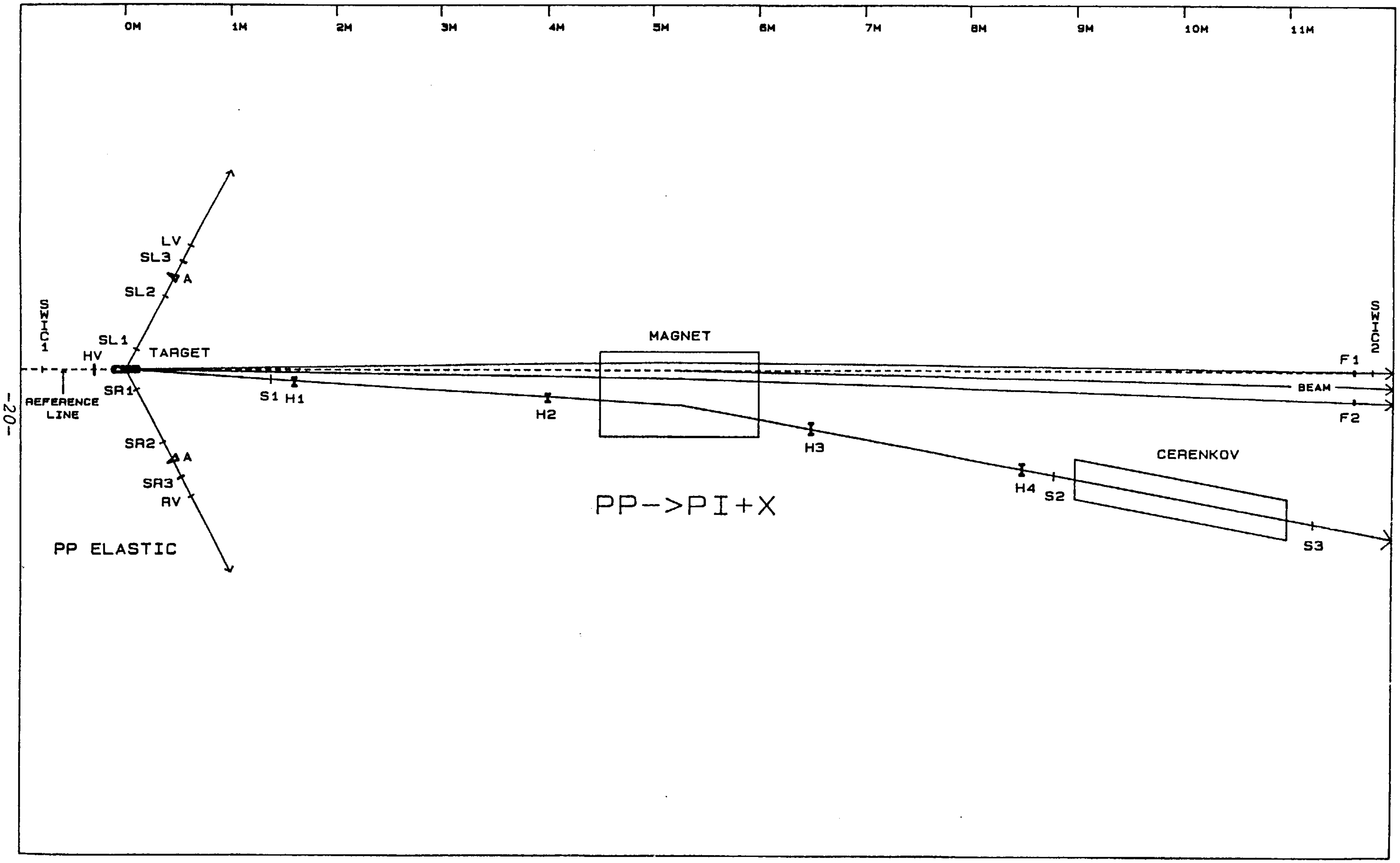

0M
1M
2M
3M
4M
5M
6M
7M
8M
9M
10M
11M
SWIC1
SWIC2
HV
REFERENCE LINE
TARGET
SL1
SL2
SL3
LV
A
SR1
SR2
SR3
RV
A
PP ELASTIC
S1
H1
H2
MAGNET
H3
H4
S2
CERENKOV
S3
F1
BEAM
F2
PP->PI+X

Figure 3

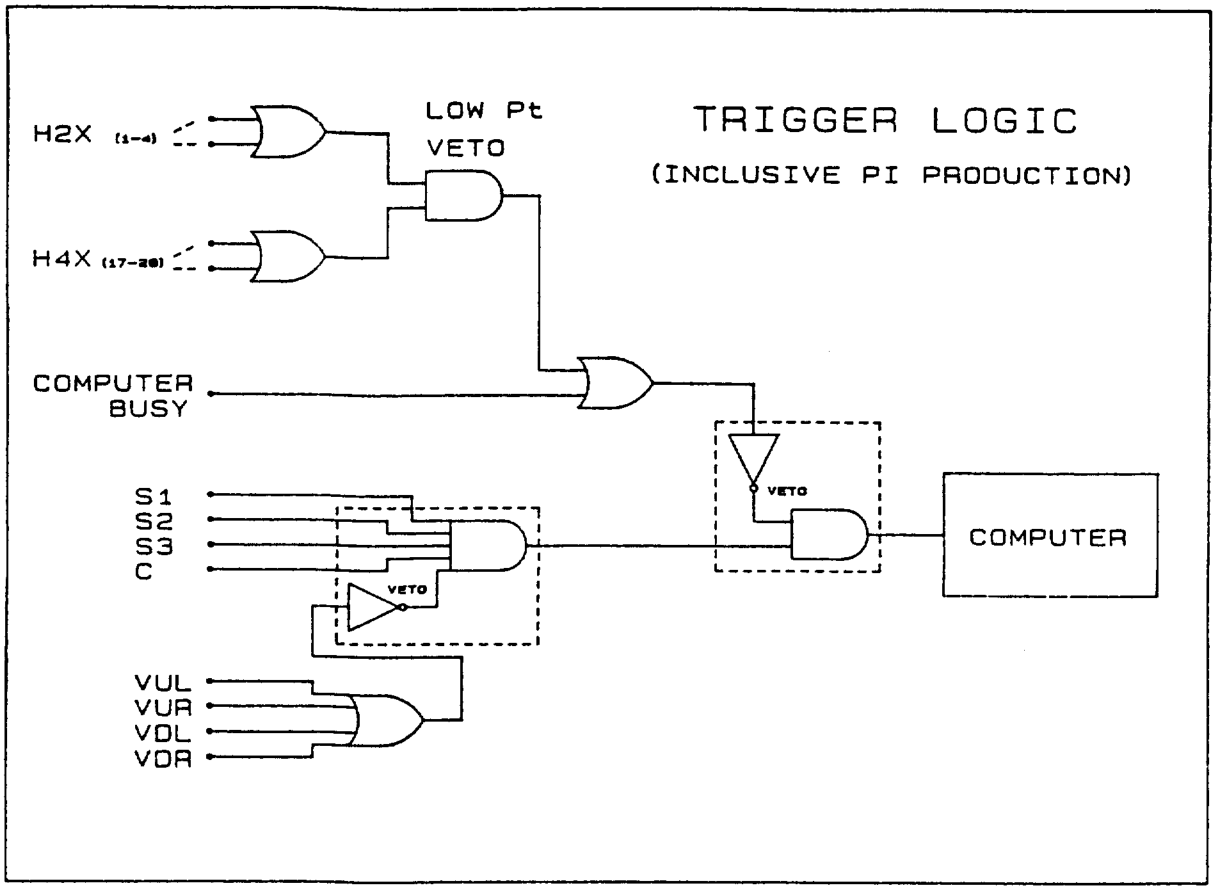

Figure 4

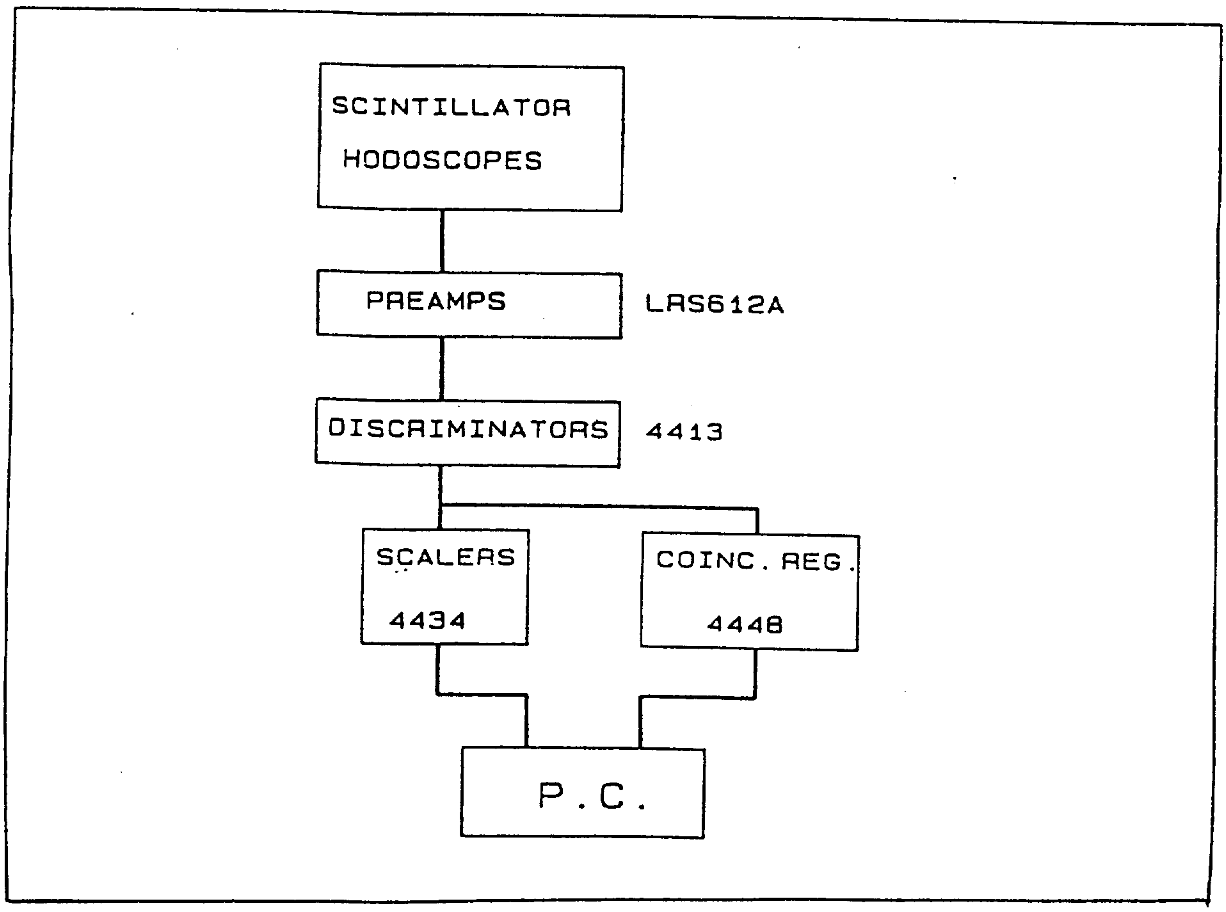

Figure 5

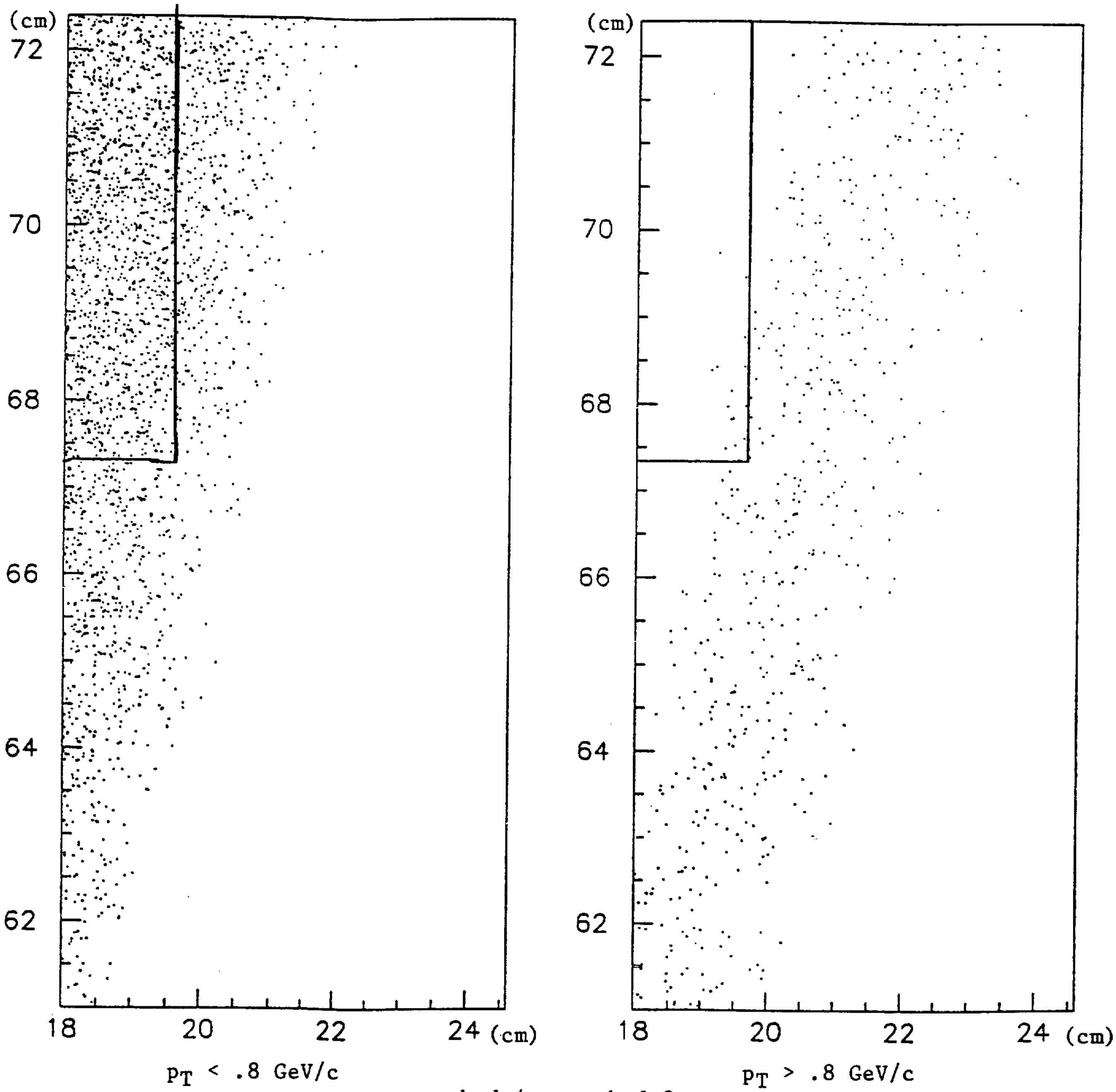

xhodo4 vs. xhodo2

Figure 6

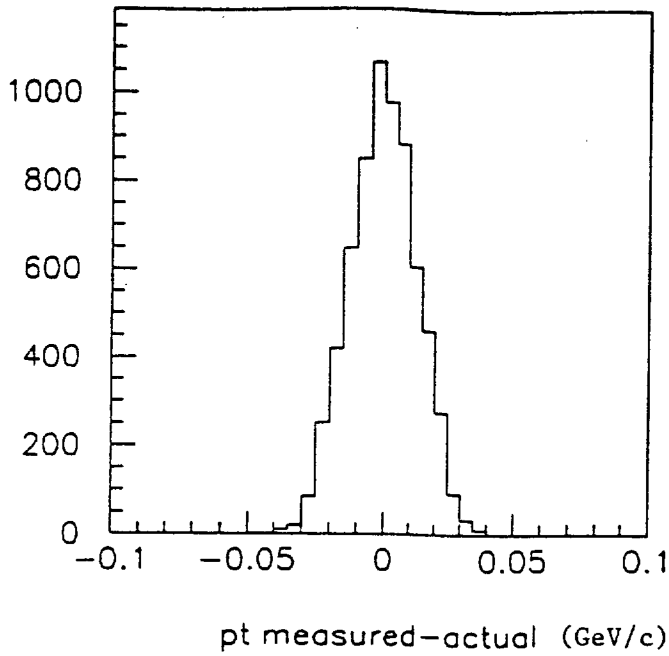

Figure 7

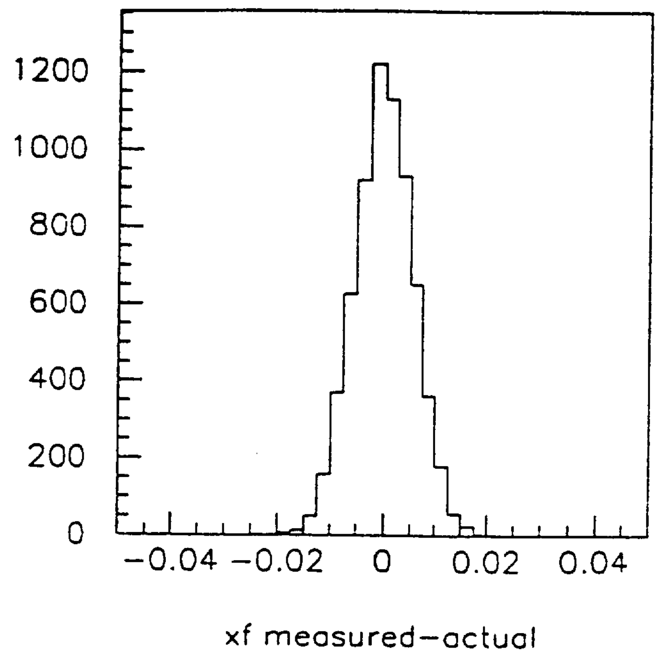

Figure 8

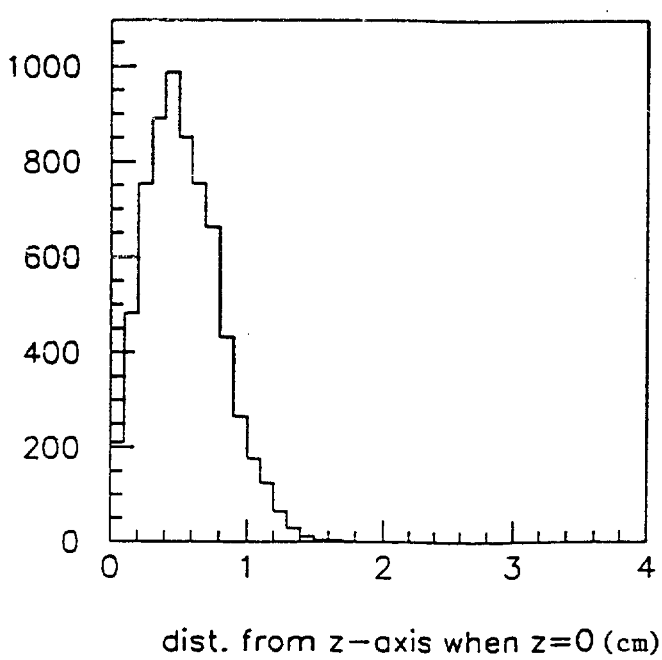

Figure 9

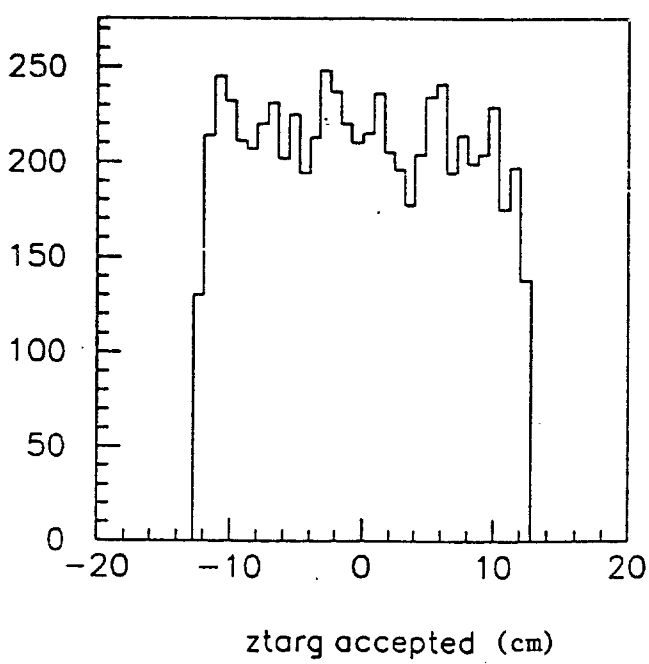

Figure 10

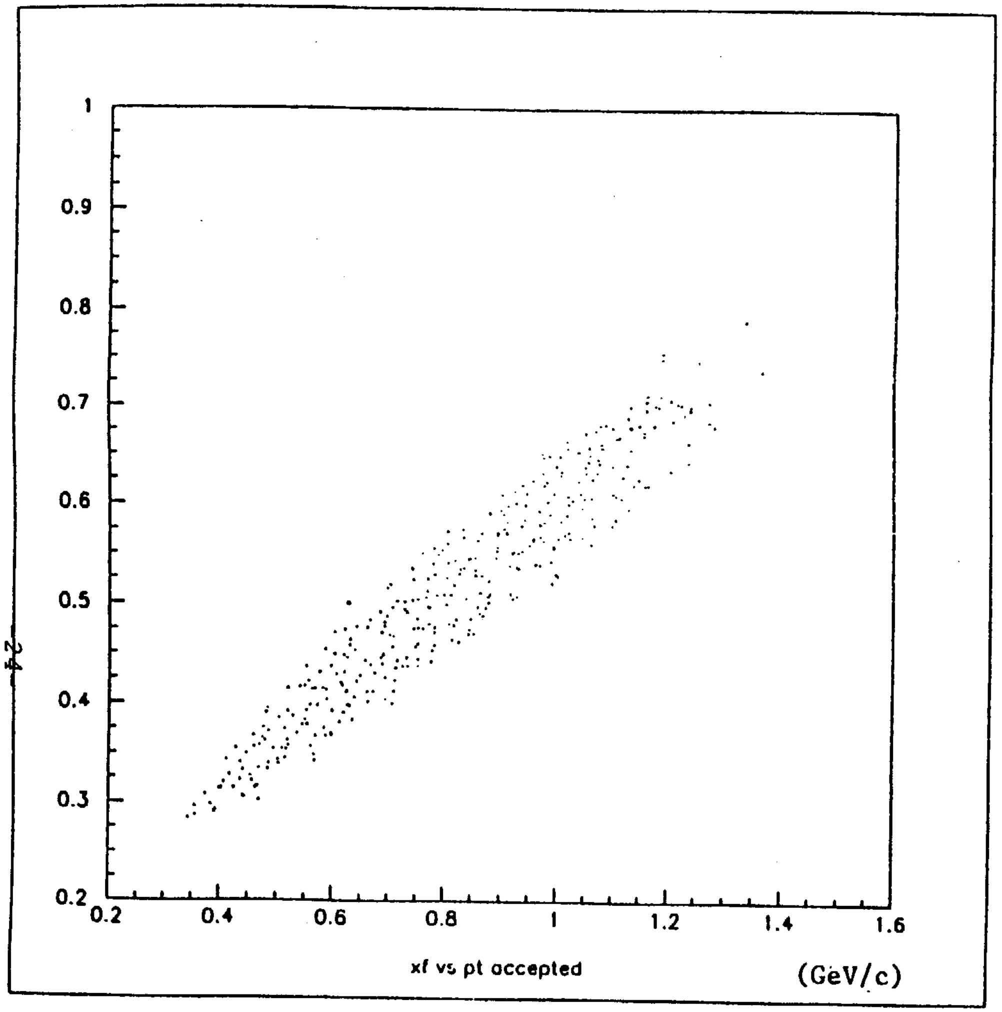

Figure 11

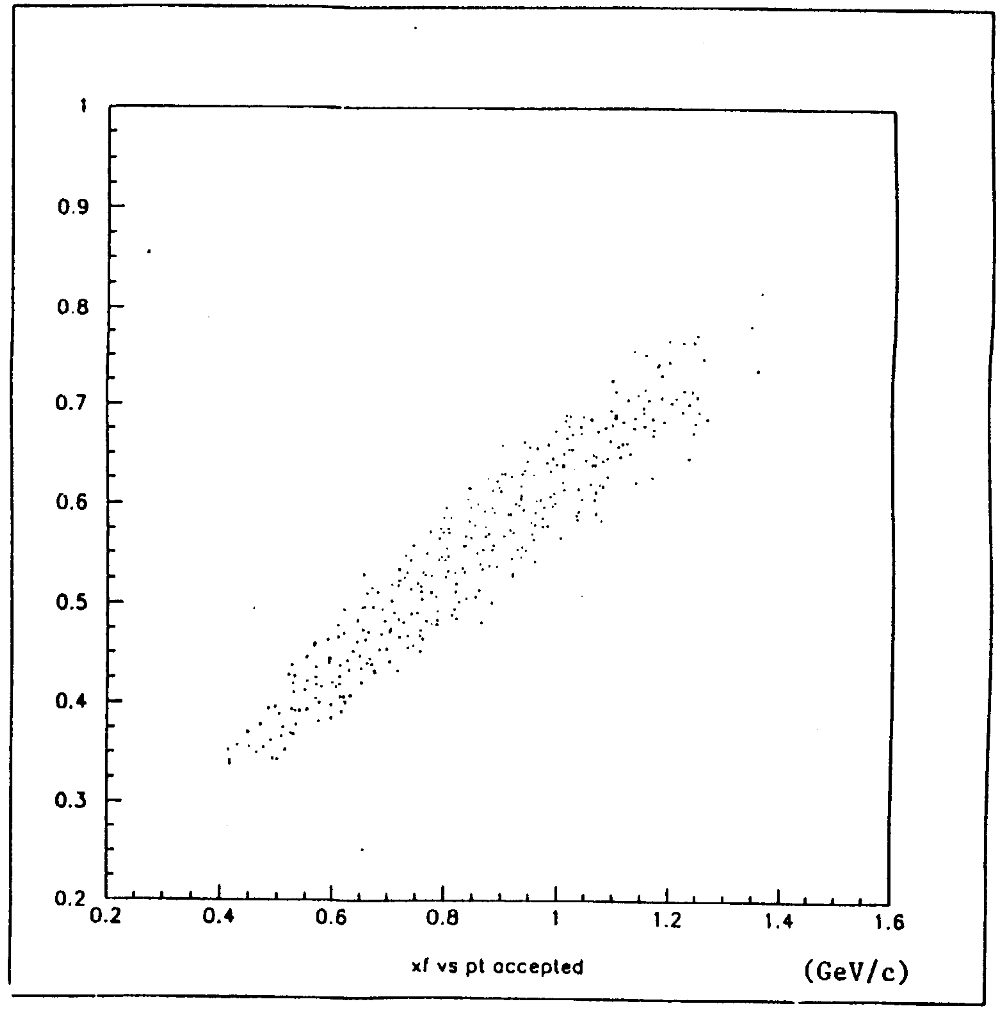

Figure 12

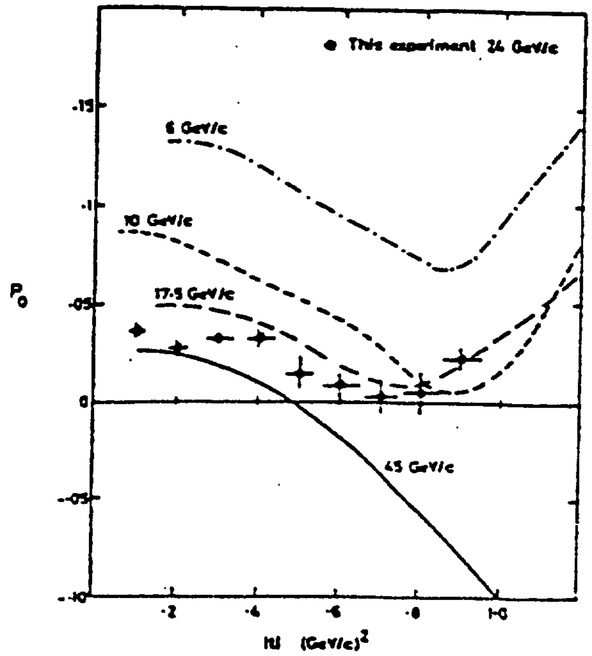

. Polarization in pp elastic scattering at 24 GeV/c. The curves are "visual fits" of the data at 6, 10, 17.5 and 45 GeV/c from refs. [2,3].

Figure 13

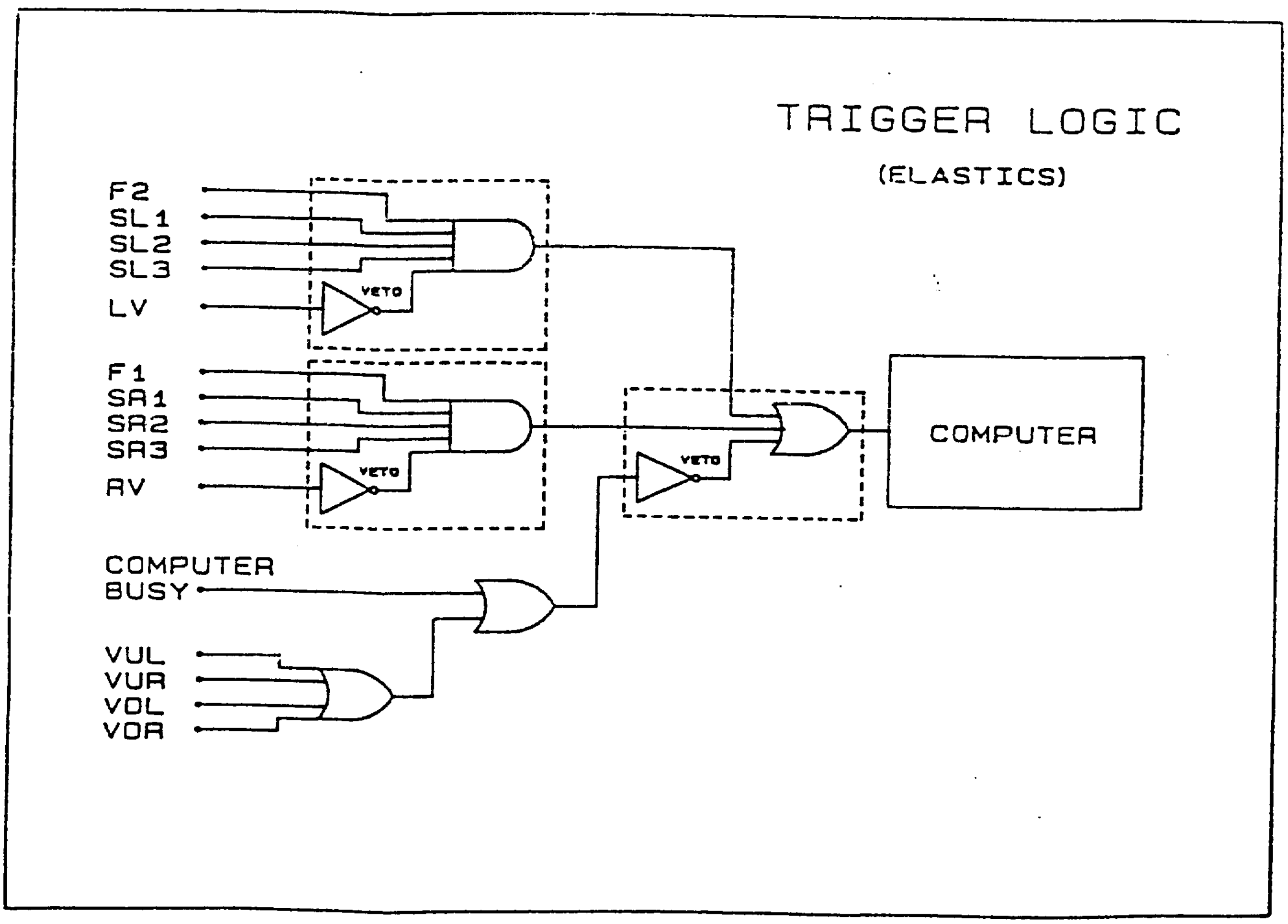

Figure 14